KSME

Springer

Journal of Mechanical Science and Technology 37 (11) 2023

Original Article
DOI 10.1007/s12206-023-1018-0

Keywords:
· Printed electronics
· Roll-to-roll process
· Contact pressure uniformization
· Measurement time-delay
· Print quality

Correspondence to:
Dongho Oh
dongho@cnu.ac.kr

Citation:
Kim, D., Kim, Y., Kim, H., Kim, J., Kang, J., Choi, Y., Oh, D. (2023). Individual drive cross-coupled control system to compensate for measurement time-delay for roll-to-roll contact pressure uniformization. Journal of Mechanical Science and Technology 37 (11) (2023) 5789~5795. http://doi.org/10.1007/s12206-023-1018-0

Received July 5th, 2023
Revised August 8th, 2023
Accepted August 8th, 2023

† Recommended by Editor
No-cheol Park

© The Korean Society of Mechanical Engineers and Springer-Verlag GmbH Germany, part of Springer Nature 2023

Individual drive cross-coupled control system to compensate for measurement time-delay for roll-to-roll contact pressure uniformization

Daehyeon Kim, Youngjin Kim, Hyeongrae Kim, Juyeon Kim, Jongmo Kang, Yuchang Choi and Dongho Oh

Department of Mechanical Engineering, Chungnam National University, 99 Daehak-ro, Yuseong-gu, Daejeon 34134, Korea

Abstract As the market demand for products such as flexible displays, IoT devices, and healthcare devices increases, attention has been drawn to printed electronics by a roll-to-roll process that can continuously produce electronic products on flexible substrates using functional inks. In particular, printed patterns need to be uniform in terms of the line width and thickness, which requires uniform control of the contact pressure during the roll-to-roll process, in processes that require ultra-fine pattern printing such as thin-film transistors for flexible displays. Because the contact pressure is indirectly measured using load cells, the performance of the conventional contact pressure control method tends to deteriorate due to the occurrence of time-delay and magnitude errors. Using the transfer function between the actual contact pressure and load cell, the time-delay is measured and compensated. To achieve contact pressure uniformization, the individual drive cross-coupled control system with the time-delay compensation is proposed.

1. Introduction

Printed electronics by the roll-to-roll process can be applied to various electronic components and products, including thin-film transistors (TFTs) for flexible displays, internet of things (IoT) devices, healthcare devices, and radio-frequency identification components [1, 2]. The process supports large-scale and continuous production, making it particularly suitable for low-cost, high-speed, and large-scale production. Many technologies for print quality improvement have been extensively studied to commercialize printed electronics. More recently, some processes capable of ultra-fine patterning, such as the roll-to-roll reverse offset and the roll-to-roll nanoimprint, have been highlighted [3, 4]. Control technologies that can improve the print quality include contact pressure control, web position control, and tension control. The web position error can be caused by the speed difference between the rotational motion of the roll and the linear motion of the web, and the tension error can be caused by temperature disturbance during the drying process [5]. Among these technologies, the contact pressure control can improve the uniformity of the line width and the thickness for a printed pattern [6].

In our previous paper, we proposed a 2-degree of freedom (DOF) individual drive system that reduces the non-uniformity of the contact pressure using two servo motors at the two ends of the impression roll [7, 8]. When the two servo motors apply pressure on the impression roll, interference at both ends can be compensated, but performance limitations are observed in this case. We found that uniform control of the contact pressure is constrained by time-delays and magnitude errors arising from a structural condition, given that the contact pressure is indirectly measured using a load cell. This paper proposes an individual drive cross-coupled control (CCC) system with time-delay compensation that achieves contact pressure uniformization.

The proposed roll-to-roll individual drive system is the CCC-based control system by measuring the transfer function between the load cell and the nip that is the actual contact surface of

the roll. The transfer function, which can be derived by performing an impact test on the contact surface of the roll, may cause time-delay. The measured time-delay can be compensated using the time-delay predictor to minimize the effect of the time-delay [9]. We performed experiments to verify the proposed individual drive CCC system with time-delay compensation.

2. Individual drive cross-coupled control system with time-delay compensation

2.1 System configuration

Figs. 1 and 2 illustrate the roll-to-roll system in which servo motors apply force on the impression roll, which applies pressure on the plate roll along the linear-motion guide. In general, the contact pressure can be measured using a pressure-measuring film or force-sensing resistor. However, when the roll-to-roll system is in actual printing, continuous measurement is not possible due to several constraints, such as the area of the pressure measurement film and the data transmission of the force sensing resistor. To resolve this issue, two load cells are attached at both ends of the impression roll to measure the pressure, and the actual contact surface and the position where the pressure is measured are different. Because this is an indirect method of measuring contact pressure, it is affected by the time-delay error and offers only limited improvements in the print quality.

Figs. 1 and 2 show the system configurations of 1-DOF and 2-DOF roll-to-roll systems. As shown in Fig. 1, the roll-to-roll 1-DOF system relies on a single servo motor, and the eccentricity caused by the precision errors complicates the uniform control of the contact pressure. In Fig. 2, the roll-to-roll 2-DOF system has two servo motors that ensure more uniformity compared to the 1-DOF system. However, the force applied by the servo motors influences the force at the other end, and this must be considered to ensure that the contact pressure is uniform.

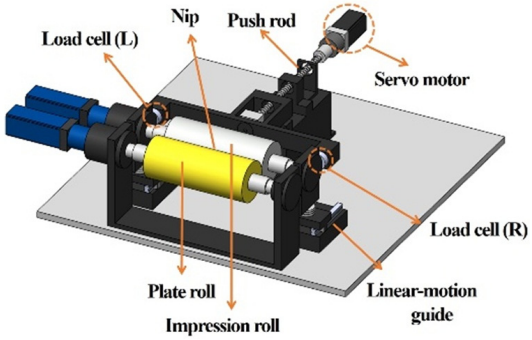

Fig. 1. Roll-to-roll 1-DOF servo drive system.

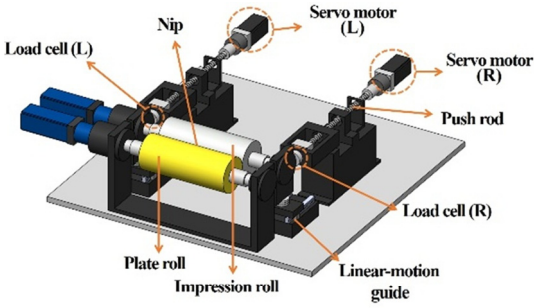

Fig. 2. Roll-to-roll 2-DOF servo drive system.

2.2 Roll shape measurement by repeatable run-out

The eccentricity caused by manufacturing errors as shown in Fig. 3 needs to be resolved for contact pressure uniformization. The eccentricity is estimated using a laser displacement sensor and a gap sensor at the top of the roll, as shown in Fig. 4, to divide the rotational axis of the impression roll and plate roll into 25 points to measure repeatable run-out. The repeatable run-out, which may occur due to assembly errors and/or precision errors in roll manufacturing, is a kind of periodic vibration error caused by the roll rotation. Then, to measure the time-delay value, the impact test is performed at the nip close to the R-axis.

From the measurements, the maximum run-out values are 13.9 μm for the impression roll and 10.7 μm for the plate roll. Figs. 5 and 6 present the repeatable run-out components of the impression roll and plate roll. The phase difference in the contact surface of the roll for 25 points in the direction of the rota-

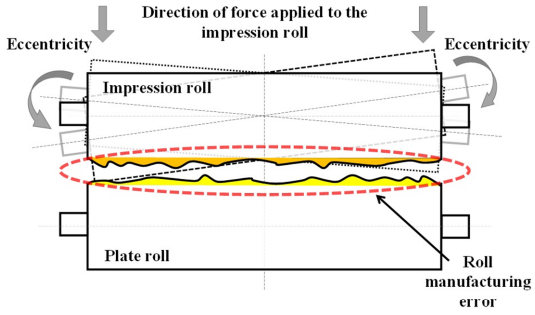

Fig. 3. Eccentricity due to manufacturing errors.

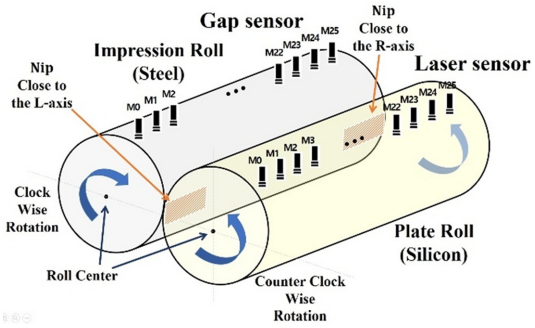

Fig. 4. Sensor placement for roll shape measurement.

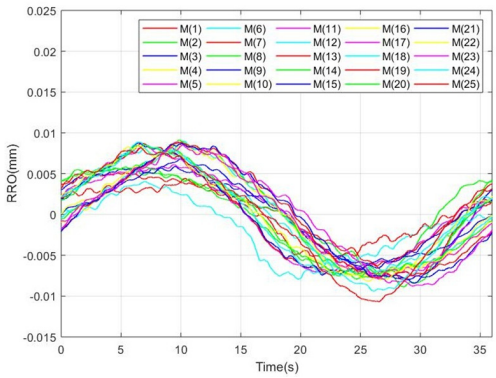

Fig. 5. Repeatable run-out of the impression roll.

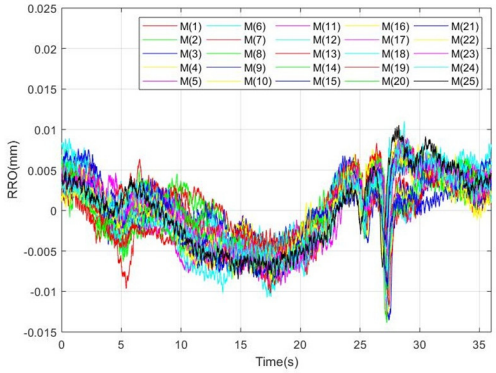

Fig. 6. Repeatable run-out of the plate roll.

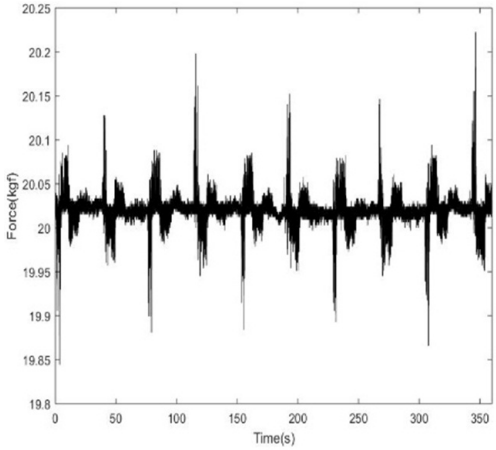

Fig. 7. Contact force measured by the load cell.

tional axis is confirmed, and assembly and precision errors can be estimated.

2.3 Time-delay measurement

The contact force measured by the load cell is given in Fig. 7. Because the contact force is indirectly measured, there is a high probability of time-delay errors, which affects the uniformity of the contact pressure [10]. Accurate time-delay values are

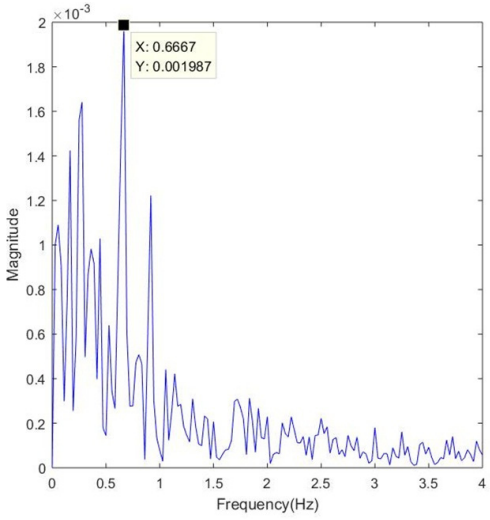

Fig. 8. Spectral density function of load cell signal.

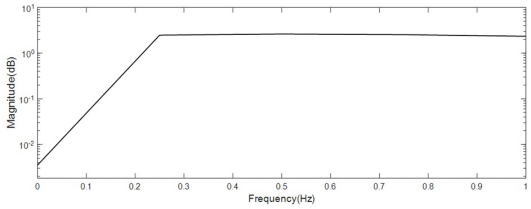

(a)

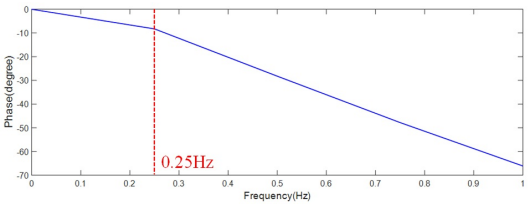

(b)

Fig. 9. Frequency response function between load cell (L) and nip (R): (a) magnitude; (b) phase.

generally able to be estimated by means of a frequency analysis or by cross-correlation of the load cell signal. The contact force expressed in the form of the spectral density function is shown in Fig. 8. According to the rotational frequency of a roll of about 0.67 Hz, the frequency band of interest with a relatively large magnitude is 1 Hz or less.

To determine the relationship between the indirectly measured force by the load cell and the actual pressure applied to the roll, some impacts were applied at the nip close to the L-axis and the R-axis of the impression roll. Based on the relationship, four time-delays were measured between the two nips, which were close to the L-axis and the R-axis, the two load cells which are the load cell (L) and the load cell (R). Two frequency response functions are shown in Figs. 9 and 10, which were acquired by repeating the test ten times.

According to the Fourier transform, the time-delay is given by the gradient of the phase, as expressed in Eq. (1). The time-

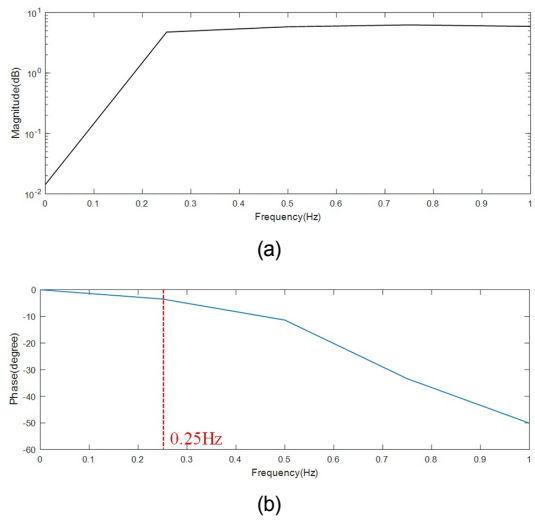

Fig. 10. Frequency response function, between load cell (R) and nip (R): (a) magnitude; (b) phase.

delay was measured by analyzing the phase, as shown in Figs. 9(b) and 10(b). Here, f is the rotational frequency of the roll, τ is the time-delay value, and $\phi(f)$ is the phase of the rotational frequency. We obtained a phase graph from the frequency response function and calculated the gradient, ∇f, of the phase graph in a linear interval of 0 Hz to 0.25 Hz. According to the phase measured from the nip close to the L-axis, the gradient was 0.578, and the time-delay was 91.99 ms. From the nip close to the R-axis, the gradient was 0.243, and the time-delay was 38.74 ms.

$$F\left[x(t-\tau)\right]=\int_{-\infty}^{\infty}x(t-\tau)e^{-j\omega t}dt$$
$$=e^{-j\omega\tau}\int_{-\infty}^{\infty}x(t)e^{-j\omega t}dt=X(j\omega)e^{-j\omega\tau}=X(j\omega)e^{-j2\pi f\tau} \quad (1)$$

$$\phi(f)=-2\pi\tau f=\nabla f\cdot f\rightarrow\tau=-\nabla f/2\pi\,. \quad (2)$$

2.4 Time-delay compensation

To compensate for the measurement time-delay, we employed the time-delay predictor proposed by Smith. The time-delay predictor uses feedback signals separated from the time-delay part and magnitude part of the transfer function. Fig. 11 shows the time-delay compensator designed with a 1-DOF single-input and single-output (SISO) system to exclude the effect of the time-delay. As a typical controller, we used a PID controller for pole assignment, where 'Ref' means the desired contact pressure to be uniformly controlled. The model of 'motor' was a Yaskawa SGM7A servo motor.

However, a multiple-input and multiple-output (MIMO) system had to be considered in our 2-DOF roll-to-roll system. As shown in Fig. 12, we proposed the individual drive CCC system with time-delay compensation for uniformizing contact pressure by applying the time-delay compensator to the MIMO system.

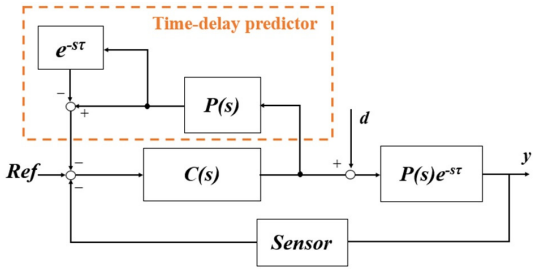

Fig. 11. Time-delay compensation in SISO control system.

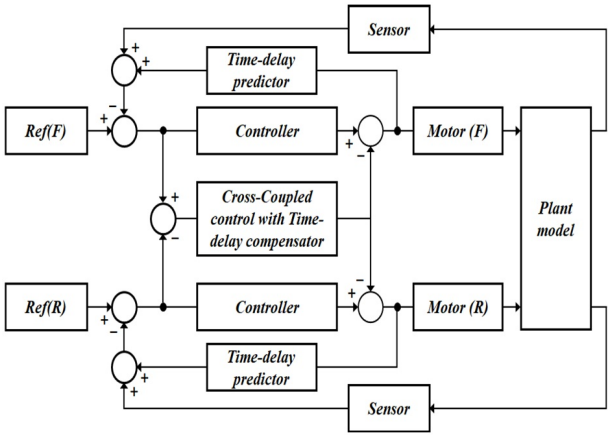

Fig. 12. Individual drive cross-coupled control system with time-delay compensation.

3. Contact pressure estimation model

Improving print quality is limited when using the method of measuring the contact pressure by attaching a load cell onto both ends of the impression roll, as a time-delay occurs due to the characteristics of the structure. The relationship between the impression roll and the plate roll was modeled as a state-space equation in consideration of the actual contact pressure, the force measured by the load cell, and relative displacement between the impression roll and plate roll.

As shown in Fig. 13, the roll-to-roll model considering the contact pressure behaves similarly to the half-car model with regard to describing the relationship between the impression roll and the plate roll while servo motors are acting on the impression roll [11]. The equation of motion in the perpendicular direction is expressed as Eq. (7), and the equation of motion for the pitch moment is Eq. (8). Substituting the constraint equations from Eqs. (3)-(6) into Eqs. (7) and (8) leads to Eqs. (9) and (10). The state-space equations Eqs. (11) and (12) are subsequently derived and are then expressed in matrix form, as given by Eqs. (18)-(25). Eq. (15) shows the relative displacement between the impression roll and plate roll, Eq. (16) shows the contact pressure between the impression roll and plate roll, and Eq. (17) shows the force measured by the load cell.

$$L=L_{l1}+L_{r1} \quad (3)$$

Table 1. Description of model parameters in Fig. 13.

L_{l1}, L_{r1}	Distance from the center of the impression roll to both ends
L_{l2}, L_{r2}	Distance from the center of the impression roll to the repeatable run-out measurement point
X_{Pl}, X_{Pr}	Run-out of plate roll
X_{il}, X_{ir}	Run-out of impression roll
X_{Sl}, X_{Sr}, X_S	Relative displacement between the impression roll and plate roll
F_{ml}, F_{mr}	Force applied to the impression roll (measured force on the load cell)
F_l, F_r	Contact pressure between the impression roll and plate roll
m_i, m_p	Mass of impression roll and plate roll
I_i, θ_i	Moment of inertia of rotation of impression roll, rotation angle of impression roll
c , k	Damping of roll surface, rigidity of roll surface

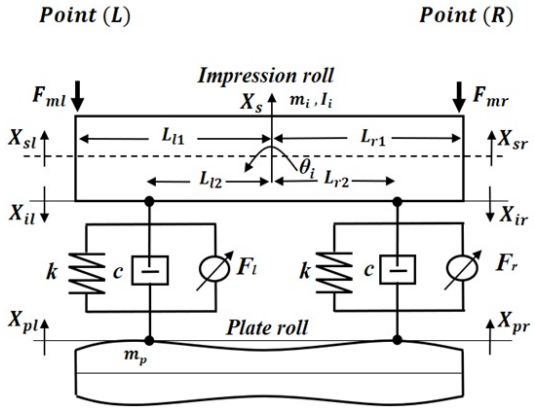

Fig. 13. Roll-to-roll contact pressure estimation model.

$$L_s = L_{l2} + L_{r2} \tag{4}$$

$$X_s = \left(L_{r2}X_{sl} + L_{l2}X_{sr}\right)/L \tag{5}$$

$$\theta_i = \left(X_{sr} - X_{sl}\right)/L \tag{6}$$

$$\begin{aligned} &m_i\ddot{X}_s + c\left(\dot{X}_{sl} + \dot{X}_{sr}\right) + k\left(X_{sl} + X_{sr}\right) \\ &-F_{ml} - F_{mr} + F_l + F_r = 0 \end{aligned} \tag{7}$$

$$\begin{aligned} &I_i\ddot{\theta}_i - L_{l2}\left(c\dot{X}_{sl} + kX_{sl} + F_l\right) + L_{r2}\left(c\dot{X}_{sr} + kX_{sr} + F_r\right) \\ &-L_{l1}F_{ml} + L_{r1}F_{mr} = 0 \end{aligned} \tag{8}$$

$$\begin{aligned} &\frac{m_i}{L}\left(L_{r2}\ddot{X}_{sl} + L_{l2}\ddot{X}_{sr}\right) + c\left(\dot{X}_{sl} + \dot{X}_{sr}\right) + k\left(X_{sl} + X_{sr}\right) \\ &-F_{ml} - F_{mr} + F_l + F_r = 0 \end{aligned} \tag{9}$$

$$\begin{aligned} &\frac{I_i}{L}\left(\ddot{X}_{sr} - \ddot{X}_{sl}\right) - L_{l2}\left(c\dot{X}_{sl} + kX_{sl} + F_l\right) \\ &+L_{r2}\left(c\dot{X}_{sr} + kX_{sr} + F_r\right) - L_{l1}F_{ml} + L_{r1}F_{mr} = 0 \end{aligned} \tag{10}$$

$$\begin{aligned} \ddot{X}_{sl} = &\left(-\frac{cLL_{l2}^{\ 2}}{L_sI_i} - \frac{cL}{mL_s}\right)\dot{X}_{sl} + \left(\frac{cLL_{l2}L_{r2}}{L_sI_i} - \frac{cL}{mL_s}\right)\dot{X}_{sr} \\ &+\left(-\frac{kLL_{l2}^{\ 2}}{L_sI_i} - \frac{kL}{mL_s}\right)X_{sl} + \left(\frac{kLL_{l2}L_{r2}}{L_sI_i} - \frac{kL}{mL_s}\right)X_{sr} \\ &+\left(-\frac{LL_{l1}L_{l2}}{L_sI_i} + \frac{L}{mL_s}\right)F_{ml} + \left(\frac{LL_{r1}L_{l2}}{L_sI_i} + \frac{L}{mL_s}\right)F_{mr} \\ &+\left(-\frac{LL_{l2}^{\ 2}}{L_sI_i} - \frac{L}{mL_s}\right)F_l + \left(\frac{LL_{l2}L_{r2}}{L_sI_i} - \frac{L}{mL_s}\right)F_r \end{aligned} \tag{11}$$

$$\begin{aligned} \ddot{X}_{sr} = &\left(\frac{cLL_{l2}L_{r2}}{L_sI_i} - \frac{cL}{mL_s}\right)\dot{X}_{sl} + \left(-\frac{cLL_{r2}^{\ 2}}{L_sI_i} - \frac{cL}{mL_s}\right)\dot{X}_{sr} \\ &+\left(\frac{kLL_{l2}L_{r2}}{L_sI_i} - \frac{kL}{mL_s}\right)X_{sl} + \left(-\frac{kLL_{r2}^{\ 2}}{L_sI_i} - \frac{kL}{mL_s}\right)X_{sr} \\ &+\left(\frac{LL_{l1}L_{r2}}{L_sI_i} + \frac{L}{mL_s}\right)F_{ml} + \left(-\frac{LL_{r1}L_{r2}}{L_sI_i} + \frac{L}{mL_s}\right)F_{mr} \\ &+\left(\frac{LL_{l2}L_{r2}}{L_sI_i} - \frac{L}{mL_s}\right)F_l + \left(\frac{LL_{r2}^{\ 2}}{L_sI_i} - \frac{L}{mL_s}\right)F_r \end{aligned} \tag{12}$$

$$\dot{x} = \mathrm{A}x + \mathrm{B}u + \mathrm{E}f \tag{13}$$

$$y = \mathrm{C}f \tag{14}$$

$$x = \begin{bmatrix} \dot{X}_{sl} & \dot{X}_{sr} & X_{sl} & X_{sr} \end{bmatrix}^T \tag{15}$$

$$f = \begin{bmatrix} F_l & F_r \end{bmatrix}^T \tag{16}$$

$$u = \begin{bmatrix} F_{ml} & F_{mr} \end{bmatrix}^T \tag{17}$$

$$A = \begin{bmatrix} A_1 & A_2 \\ A_3 & A_4 \end{bmatrix} \tag{18}$$

$$A_1 = \begin{bmatrix} -\frac{cLL_{l2}^{\ 2}}{L_sI_i} - \frac{cL}{mL_s} & \frac{cLL_{l2}L_{r2}}{L_sI_i} - \frac{cL}{mL_s} \\ \frac{cLL_{l2}L_{r2}}{L_sI_i} - \frac{cL}{mL_s} & -\frac{cLL_{r2}^{\ 2}}{L_sI_i} - \frac{cL}{mL_s} \end{bmatrix} \tag{19}$$

$$A_2 = \begin{bmatrix} -\frac{kLL_{l2}^{\ 2}}{L_sI_i} - \frac{kL}{mL_s} & \frac{kLL_{l2}L_{r2}}{L_sI_i} - \frac{kL}{mL_s} \\ \frac{kLL_{l2}L_{r2}}{L_sI_i} - \frac{kL}{mL_s} & -\frac{kLL_{r2}^{\ 2}}{L_sI_i} - \frac{kL}{mL_s} \end{bmatrix} \tag{20}$$

$$A_3 = \begin{bmatrix} 1 & 0 \\ 0 & 1 \end{bmatrix} \tag{21}$$

$$A_4 = \begin{bmatrix} 0 & 0 \\ 0 & 0 \end{bmatrix} \tag{22}$$

$$B = \begin{bmatrix} -\frac{LL_{l1}L_{l2}}{L_sI_i} + \frac{L}{mL_s} & \frac{LL_{r1}L_{l2}}{L_sI_i} + \frac{L}{mL_s} \\ \frac{LL_{l1}L_{r2}}{L_sI_i} + \frac{L}{mL_s} & -\frac{LL_{r1}L_{r2}}{L_sI_i} + \frac{L}{mL_s} \\ 0 & 0 \\ 0 & 0 \end{bmatrix} \tag{23}$$

$$E = \begin{bmatrix} -\frac{LL_{l2}^{\ 2}}{L_sI_i} - \frac{L}{mL_s} & \frac{LL_{l2}L_{r2}}{L_sI_i} - \frac{L}{mL_s} \\ \frac{LL_{l2}L_{r2}}{L_sI_i} - \frac{L}{mL_s} & \frac{LL_{r2}^{\ 2}}{L_sI_i} - \frac{L}{mL_s} \\ 0 & 0 \\ 0 & 0 \end{bmatrix} \tag{24}$$

$$C = \begin{bmatrix} 1 & 0 \\ 0 & 1 \end{bmatrix}. \tag{25}$$

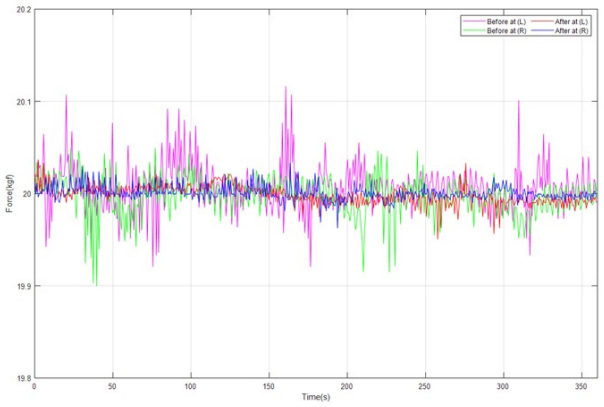

Fig. 14. Comparison between before and after time-delay MIMO compensation.

4. Experimental verification of contact pressure uniformization

Because the contact forces from the servo motors interfere with each other and affect the uniform control of the contact pressure, we designed the proposed individual drive CCC system to compensate for the interference caused by the two servo motors. Several experiments were conducted to investigate the performance of the time-delay compensator in the individual drive CCC system. As for the experimental conditions, the driving speed of the roll motor was maintained at 1.67 rpm, and the desired contact force value was set at 20 kgf, which is the industrial nominal contact force.

Fig. 14 shows the comparison between controlling the contact pressure using the CCC system without time-delay compensation (before) and the CCC system with time-delay compensation (after). The minimum-maximum contact pressure difference dropped from 0.2165 kgf (for a maximum of 20.1163 kgf and a minimum of 19.8998 kgf) before compensation to 0.0701 kgf (for a maximum of 20.0329 kgf and minimum of 19.9628 kgf) after compensation. The standard deviation of the contact pressure error was reduced by 67 % from 0.024613 kgf to 0.00803 kgf, indicating that the contact pressure was becoming more uniformed and corrected by the journal office.

5. Conclusions

In this paper, we have proposed an individual drive CCC system to uniformize contact pressure to enhance the print quality of the roll-to-roll process for printed electronics. When the pressure by the servo motor is applied to both ends of the impression roll, one force affects the other side in the 2-DOF roll-to-roll system proposed in our previous work. We designed the proposed individual drive CCC system to compensate for the influence between the two motors and to improve the control performance. However, since the contact pressure is indirectly measured using load cells at the end of the impression roll in the individual drive CCC system, a time-delay occurs between the actual contact pressure and the load cell. In addition, the effect of time-delay is more complicated than in an SISO system because it is a MIMO system composed of 2-input and 2-output. We measured the time-delay values of four paths between the actual contact force and the load cell and performed the time-delay compensation in the MIMO system using the time-delay predictor. We verified contact pressure uniformization by the individual drive CCC system with time-delay compensation through several experiments.

Recently, the roll-to-roll reverse offset technology in printed electronics processes has been emerging and is being found suitable for production in various flexible products: not only flexible and/or large display panels, IoT devices, radio-frequency identification components, and healthcare devices but also the backplane TFT that matches the characteristics of the flexibility of the substrate. However, flexible TFTs using the current level of printing technology has limitations in satisfying specification requirements because the backplane of LCD and OLED displays requires high charge mobility [12]. To solve this limitation, it is necessary to ensure technology for ultra-fine patterning and for uniformizing printing contact pressure. Therefore, the proposed individual drive CCC system with time delay compensation will contribute to the next-generation electronic device-related market.

Acknowledgments

This work was supported by the mid-career researchers program through the national research foundation of Korea (NRF), funded by the Ministry of Science and ICT (No. 2022R1A2C 2006431123148209264 0102).

References

[1] J. U. Park and J. S. Park, The present status and future aspects of the market for printed electronics, *The Korea Institute of Information and Communication Engineering*, 17 (2) (2013) 263-272.

[2] Y. Y. No, H. Han, G.-T. Bae, A.-R. Jo and H.-M. Lee, Print backplane TFT development trend and outlook for flexible display, *Information Display*, 11 (6) (2010) 2-11.

[3] Y. M. Choi, E. S. Lee and T. M. Lee, Mechanism of reverse-offset printing, *Micromechanics and Micro Engineering*, 25 (7) (2015).

[4] S. H. Ahn and L. J. Guo, Large-area roll-to-roll and roll-to-plate nanoimprint lithography: a step toward high throughput application of continuous nanoimprinting, *ACS Nano* (2009) 2304-2310.

[5] C. W. Lee, H. K. Kang and K. H. Kang, A study on tension behavior considering thermal effects in roll-to-roll E-printing, *Mechanical Science and Technology*, 24 (5) (2010) 1097-1103.

[6] K. H. Choi, T. T. Thanh and H. C. Kim, On a new approach for gravure/offset printing pressure control algorithm development using the full state feedback controller, *2009 IEEE International Symposium on Assembly and Manufacturing*, Seoul, Korea (2009) 88-94.

[7] J. M. Park, Y. J. Kim and H. R. Kim, Contact printing pressure uniformization in roll-to-roll process using individual drive cross-coupled torque control, *Microsystem Technologies*, 27 (2021) 2515-2522.
[8] J. H. Kim, Y. J. Kim and T. H. Kim, Printing pressure uniformization through adaptive feedforward control in roll-to-roll printing process, *Microsystem Technologies*, 26 (1) (2020) 265-273.
[9] S. S. Yeh and P. L. Hsu, Estimation of the contouring error vector for the cross-coupled control design, *IEEE/ASME Transactions on Mechatronics*, 7 (1) (2002) 44-51.
[10] Y. D. Chen, P. C. Tung and C. C. Fuh, Modified smith predictor scheme for periodic disturbance reduction in linear delay systems, *Process Control*, 17 (10) (2006) 799-804.
[11] H. J. Choi and S. Jung, Design of a time-delay compensator using neural network in a tele-operation system, *The Korean Institute of Intelligent Systems*, 21 (4) (2011) 449-455.
[12] P. Gandhi, S. Adarsh and K. I. Ramachandran, Performance analysis of half car suspension model with 4 DOF using PID, LQR, FUZZY and ANFIS controllers, *Procedia Computer Science*, 115 (2017) 2-13.
[13] E. Jung, S. J. Kim and S. M. Cho, Production technology status of organic lighting and display via roll-to-roll process, *Vacuum Magazine*, 4 (2) (2017) 24-28.

Dongho Oh received his B.S. from Hanyang University, Seoul, Korea, in 1989 and his M.S. and Ph.D. from the KAIST (Korea Advanced Institute of Science and Technology), Korea, in 1991 and 1996, respectively. Currently, he is Professor of Mechanical Engineering at Chungnam National University in Korea. His major research interests include the field of vibration and control of dynamic systems and fault diagnosis of mechanical systems.

Daehyeon Kim is currently studying for a Master's in Mechanical Engineering, Chungnam National University. His research interests include dynamics, position and contact pressure control system in roll-to-roll process system.